

## A Study on the Recovery of Radiation Hardening of PWR Pressure Vessel Steel Using Microhardness and Positron Annihilation

Seong Je-Garl\* and Young Ku Yoon

Korea Advanced Institute of Science and Technology

Soon Pil Choi

Korea Atomic Energy Research Institute

Yong Ki Park

Korea Standards Research Institute

(Received April 30, 1990)

### 미세경도와 양전자 소멸을 이용한 PWR 압력용기강의 조사 경화 회복에 관한 연구

제갈성·윤용구

한국과학기술원

최순필

한국원자력연구소

박용기

한국표준연구소

(1990. 4. 30 접수)

### Abstract

A post-irradiation annealing study was conducted with use of reactor pressure vessel(RPV) steel A533B Cl.1 base metal irradiated to a dose of  $4.84 \times 10^{18}$  n/cm<sup>2</sup> at about 380 °C. Microhardness and positron annihilation (PA) methods were used to obtain better understanding of the recovery of radiation hardening. Isochronal anneal experiments indicated that two recovery processes occur during annealing of irradiated specimens. The first recovery process occurs in the temperature range of 280–305°C. Microhardness and positron annihilation (PA) methods were used to obtain better understanding of the recovery of radiation hardening. Isochronal anneal experiments indicated that two recovery processes occur during annealing of irradiated specimens. The first recovery process occurs in the temperature range of 280–305°C. The variations of  $I_p$ ,  $I_w$  and  $R$  parameters indicated that the formation of vacancy clusters by vacancy agglomeration and the annihilation of monovacancies are the first recovery process. The second recovery process occurs in the range of 405–490°C and positron annihilation parameters measured indicated that the dissolution of carbon atoms decorated around vacancy-type defects and possible precipitates, and the annihilation of monovacancies

\*Presently with the Korea Electric Corporation

give rise to the second recovery process. It was further indicated that radiation anneal hardening (RAH) in the range of 305–405°C between the temperature ranges for the two processes occurs due to the formation of carbon-decorated vacancy clusters and precipitates.

The activation energies, orders of reaction and other characteristics of recovery processes were determined by the Meechan-Brinkman method. The activation energy for the first recovery process was determined as 1.76 eV and that for the second recovery process as 2.00 eV. These values are lower than those obtained by other workers. This difference may be attributed to the lower copper content of the RPV steel used in the present study.

The order of reaction for the first recovery process was determined as 1.78, while that for the second recovery process as 1.67. Non-integer orders of reaction for recovery processes seem to be attributed to the fact that several mechanisms for the first order and the second order of reaction are compounded in one process. This result also supports for the above conclusions from measurements of PA parameters.

## 요 약

약 280°C에서  $4.84 \times 10^{18} \text{ n/cm}^2$ 의 중성자 조사를 받은 원자로 압력용기강 A533B C1.1 기지금속 (base metal)을 열처리한 후, 미세경도 측정과 양전자 소멸법을 사용해서 조사경화 회복기구에 관한 더 정확한 연구를 하였다. 동시소둔 실험에 의해 2가지 회복과정이 존재한다는 것을 알 수 있었다. 첫번째 회복과정은 280–350°C 사이에서 일어나며 양전자 소멸법에 의한 몇가지 파라메타 즉, 양전자 수명, 양전자 소멸밀도(I)와  $I_p$ ,  $I_w$ , R 파라메타 값들에 의하면 이 회복과정에서 공공응집 (agglomeration of vacancies)과 단위공공의 소멸 (annihilation of monovacancies)이 일어나는 것으로 해석되었다. 또한 두번째 회복과정은 405°C 이상의 고온에서 발생하며, 양전자소멸 파라메타들은 공공형 결함 주위에 부착되었던 탄소원자의 용해, 석출물의 용해 그리고 단위공공의 소멸이 이 회복과정에서 일어나는 것으로 해석되었다. 그리고 두 회복과정의 중간 온도 영역인 305–405°C에서는 탄소가 부착된 공공결집체 (vacancy clusters)의 형성과 석출물의 형성에 의한 소둔중경화 (radiation anneal hardening)가 일어나는 것으로 해석되었다. Meechan-Brinkman 방법을 이용하여 활성화 에너지와 반응차수 및 그의 회복특성을 구하였다. 첫번째 회복과정의 활성화 에너지는 1.76eV로, 두번째 회복과정의 값은 2.00eV로 결정되었다. 이 값들은 다른 연구결과에 비해 낮은 편인데 이 차이는 이 연구에서 사용된 압력용기강의 낮은 탄소양에 의한 것으로 생각된다. 또한 첫번째 회복과정의 반응차수는 1.78로 두번째 회복과정의 반응차수는 1.67로 결정되었다. 회복과정에서의 반응차수가 정수가 아닌 것은 한 회복과정에 1차나 2차의 반응차수를 가진 몇가지 기구들이 복합되어 있기 때문인 것으로 생각된다. 이것은 양전자 소멸의 몇가지 파라메타에 의한 결과를 뒷받침한다.

## I. INTRODUCTION

Radiation-induced defects are generated in the material when the reactor pressure vessel (RPV) is

irradiated in fast neutron flux ( $E > 1 \text{ MeV}$ ). It is known that the RPV steel is radiation-hardened due to source hardening and friction hardening. The risk of brittle fracture increases when the

radiation-hardened RPV steel is subjected to pressurized thermal shock (PTS). The NRC Regulatory Guide 10CFR50, App. G, IV stipulates that the upper shelf energy (USE) surveillance specimens of 1/4 must be above 50 ft-lb. If their USE is lower than 50 ft-lb and the integrity of the RPV can not be proven by non-destructive test and fracture analysis, the Regulatory Guide 10CFR50, App. G, V.D. requires heat treatment of the RPV to recover radiation-induced embrittlement. [1] Hence better understanding of recovery mechanisms of radiation embrittled RPV is very important.

According to the previous studies, radiation embrittlement involves compounded effects of several factors such as neutron flux, fluence, irradiation temperature, microstructure and chemical composition. [2,3] Effects of radiation damage rate [4] and impurity contents of RPV steel [5-6], especially, those of Cu, Ni and P [7-9] are also known to be detrimental. Spitznagel [7] reported that the formation of copper-vacancy aggregates accounts for 70% of irradiation embrittlement of RPV steel. Previous workers also reported that recovery of radiation embrittlement occurs due to agglomeration and/or dissolution of vacancies [10], vacancy clusters [11,12], and depleted zones [13], and dissolution of impurity precipitates [9,14], and carbon decorated clusters [12,15,16].

Complex recovery processes of irradiation embrittlement, however, can not be completely analyzed by usual testing methods such as Charpy tests of NDTT and USE, tension tests, hardness and internal friction measurements. Hence additional methods that are sensitive to defect structure, namely, resistivity, positron annihilation (PA) and small angle neutron scattering (SANS) measurements are also used for the study of recovery mechanisms.

It is known that recovery is associated with compound recovery processes occurring during

annealing, with each of which an activation energy is associated. Many defects for which there exist different activation energies are regarded independently and simultaneously. [17,18] Since variations of frequency factor and order of reaction are complicated and initial activation energy spectrum is not known, it is difficult to analyze compounded recovery processes and associated recovery mechanisms. Hence recovery mechanisms can be usually studied by an analysis method for which several representative recovery processes occurring during annealing are regarded as a single activated process for convenience of its study. [19] The order of reaction is taken as the first order for easier analysis. [4,20,21] Analysis of a single activated process using the chemical rate equation, namely, the Meehan-Brinkman method [19], however, is considered to be most appropriate.

According to previous workers who have studied radiation effects with use of positron annihilation measurements, it was possible to explain recovery of radiation hardening by several mechanisms based on positron annihilation (PA) parameters as follows ;

The increase of life-time  $\tau$  and Doppler broadening peak parameter  $I_p$  and the decrease of intensity  $I$  and Doppler broadening wing parameter  $I_w$  indicate a recovery process associated with the formation of vacancy clusters by vacancy agglomeration. [22] The decrease of intensity  $I$  and peak parameter  $I_p$  and the increase of wing parameter  $I_w$  indicate a recovery process involving annihilation of monovacancies. The decrease of intensity is attributed to formation of carbon-decorated vacancy clusters, whereas the increase of intensity and the decrease of life-time are attributed to their dissolution. [12,16] The formation and the dissolution of precipitates have not been observed directly. In combination with results of transmission electron microscopy, however, the

increase of life-time and the decrease of intensity can be associated with formation of precipitates, and the decrease of life-time and the increase of intensity associated with dissolution of precipitates. [9,14,23]

Previous workers reported that there are two or three recovery processes occurring at the operating temperature of commercial reactors. [4,20,21] As opposed to most of the previous studies of recovery mechanisms based on the first order of reaction, the orders of reaction and activation energies associated with recovery processes are determined with use of chemical rate equations in the present study. Attempts were also made to study characteristics of recovery mechanisms of radiation-induced defects with use of microhardness and positron annihilation measurements after isochronal and isothermal annealing experiments.

## II. EXPERIMENTAL METHOD

### II-1. Specimen Preparation

Specimens used in this experiment are base metals of A533B Cl.1 that are the specimens taken from the first RPV surveillance test for Yeong-Gwang Nuclear Power Plant Unit 2. The irradiation temperature of the surveillance test specimens was about 280°C. The chemical composition of this RPV base metal is shown in Table 1.

Specimens were taken from 10mm×55mm Charpy test specimens and they were cut in 5mm×5mm×1mm specimens by a diamond cutter and polished on 600 grid emery paper to measure initial hardness value. All subsequent hardness specimens were also polished on 600 grid paper, PA specimens were polished on an automatic grinder with use of 600 grid emery paper, 1 μm Al<sub>2</sub>O<sub>3</sub> power and 0.05 μm Al<sub>2</sub>O<sub>3</sub> powder in sequence.

**Table 1 Chemical composition of the RPV Surveillance test specimens of Yeong-Gwang Nuclear Power Plant Unit 2.**

| Element | Chemical Composition (wt. %)        |                                       |
|---------|-------------------------------------|---------------------------------------|
|         | Surveillance Test Plate a) R 6506-1 | Surveillance Weldment Test Plate D a) |
| C       | .20                                 | .11                                   |
| Mn      | 1.50                                | 1.50                                  |
| P       | .015                                | .018                                  |
| S       | .006                                | .012                                  |
| Si      | .20                                 | .49                                   |
| Ni      | .54                                 | .11                                   |
| Mo      | .49                                 | .53                                   |
| Cr      | .16                                 | .018                                  |
| Cu      | .051                                | .029                                  |
| Al      | .020                                | .009                                  |
| Co      | .007                                | .005                                  |
| Pb      | <.001                               | <.011                                 |
| W       | <.01                                | <.01                                  |
| Ti      | .005                                | .004                                  |
| Zr      | <.002                               | <.002                                 |
| V       | <.002                               | <.002                                 |
| Sn      | .005                                | <.002                                 |
| As      | .011                                | .003                                  |
| Cb      | <.002                               | <.002                                 |
| N       | .012                                | .010                                  |
| B       | <.001                               | .001                                  |

a) Chemical analysis by Westinghouse

### II-2. Heat Treatment

#### 1. Isochronal Heat Treatment

So prepared specimens were first heat-treated isochronally to investigate the trend of change in hardness. Isochronal heat treatment was given for four hours based on the results of various experiments by D. Pachur [21]. Four hours were adequate for annealing out radiation induced defects. The heat treatment was conducted in the temperature range of 290-500°C in a salt bath to protect

from oxidation of specimens. The salt used was composed of  $\text{NaNO}_3$  and  $\text{KNO}_3$  in the ratio of 1 to 1. Its melting point is  $225^\circ\text{C}$  and heat-treatment in the temperature range of  $260\text{--}590^\circ\text{C}$  is possible with use of this salt bath.

The heat treatment of specimens for PA studies was performed at temperatures at which the recovery process was expected to change based on the results of hardness measurements. These temperatures of heat treatment were  $320^\circ\text{C}$ ,  $380^\circ\text{C}$  and  $500^\circ\text{C}$ .

The hardness value of unirradiated RPV base metal and the reference value of PA measurement were also required for comparison. For this purpose unirradiated A533B Cl.1 steel specimens were heat-treated for 4 hr at  $500^\circ\text{C}$ .

2. Isothermal Heat Treatment

Isothermal heat-treatments were conducted at  $320^\circ\text{C}$ ,  $380^\circ\text{C}$  and  $480^\circ\text{C}$  as a function of annealing time(i.e. 11 points).

For isothermal heat treatments of PA specimens, time interval at  $380^\circ\text{C}$  were taken as 20 min., 130 min., 350 min. and 700 min. in  $380^\circ\text{C}$  based on the results of isothermal hardness experiments.

II-3. Methods for Microhardness and Positron Annihilation Measurements

1. Microhardness Measurements

The Vickers micro-hardness tester (Matsuzawa model DMH-2) was used for microhardness measurements. Microhardness represents materials resistance to local indentation under certain load. This is expressed by DPH(diamond pyramid hardness), according to the following equation ;

$$DPH = \frac{2P \sin(\theta/2)}{d^2} \tag{1}$$

where P=load(kg-force)

d=average length of the indentation's diagonal(mm)

nal(mm)

$\theta$  =vertical angle between opposite faces( $136^\circ$ ).

The lengths were measured under the microscope of 400 times magnification after the specimens were fixed and applied 500g load during 15 seconds.

2. Positron Annihilation(PA) Measurements

The positron is the antimatter particle of the electron. The two particles have identical properties except for an opposite electrical charge. In mid-1960's it was experimentally established that the positron interacts sensitively with lattice defects of metals. Positrons are produced from  $\beta^+$  decaying radioactive isotopes such as  $^{22}\text{Na}$ ,  $^{56}\text{Co}$ , and  $^{44}\text{Ti}$ . Among these  $^{22}\text{Na}$  is most widely used. Penetration depth of positrons into materials depends on the maximum energy of positrons and the density of materials exposed to the positrons.[24]

If positrons having the energy of a few keV penetrate into metal, most of the penetrated positrons annihilate with electrons and this results in emission of mainly two gamma quanta of 511 keV that is equivalent to the rest mass energy of an electron or positron. Fig. 1 shows the decay

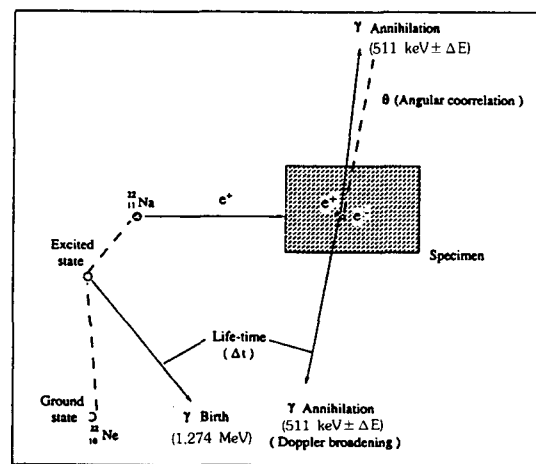


Fig. 1 The decay scheme of  $^{22}\text{Na}$  and basic principles of three types (life-time, Doppler broadening, angular correlation) of positron annihilation measurement.

scheme of  $^{22}\text{Na}$  and basic principles of three types of positron annihilation measurement, namely, positron life-time, Doppler broadening of the annihilation  $\gamma$ -ray and angular correlation.

$^{22}\text{Na}$  used frequently as a positron source emits positrons and fiducial  $\gamma$  ray of 1.274 MeV within a few picoseconds. [25] Hence the lifetime of a positron in a specimen can be determined by measuring the time delay between the birth of the fiducial  $\gamma$ -rays and that of the  $\gamma$ -ray of 511 keV.

The Doppler broadening has been demonstrated by Innes K. Mackenzie of the University of Guelph in Ontario. [26] Hence the information about the electron momentum distribution in a specimen can be obtained by measuring the energy spectrum of the annihilation  $\gamma$ -rays (line shape measurement of Doppler broadening). Since the energy of the core electrons is higher than that of free electrons, the Doppler broadening line shape becomes narrow if the number of defects such as vacancies increases.

The Doppler broadening line shape consists of two portions, namely, a central parabola attributing to annihilation of the positron-free electron pairs. These portions are defined as the peak parameter ( $I_p$ ) and the wing parameter ( $I_w$ ) as shown in Fig.2.

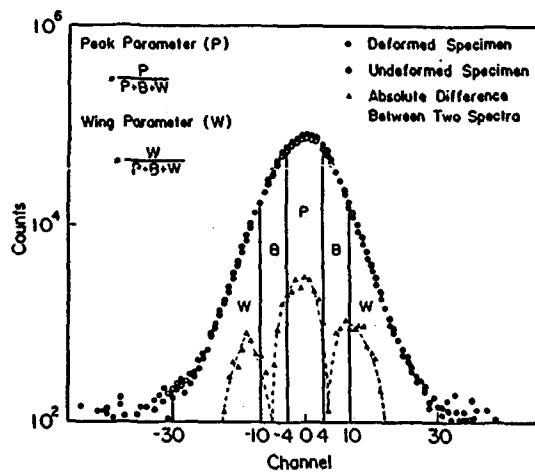


Fig. 2 Doppler broadening line shape and definition of parameters  $I_p$  and  $I_w$ .

Both the increase of  $I_p$  parameter and the decrease of  $I_w$  parameter represent an increase in the concentration of defects if the positrons are trapped by the same type of defects throughout the whole stages of deformation. Mantl and Trifshauer [27] suggested that the defect-specific parameter R can be used to resolve the information about the type of defects. The R parameter is defined with use of  $I_p$  and  $I_w$  parameter as,

$$R = \left| \frac{I_p - I_p^f}{I_w - I_w^f} \right| = \left| \frac{I_p^t - I_p^f}{I_w^t - I_w^f} \right| \quad (2)$$

where  $I_p^f$  and  $I_p^t$  are the characteristic values of the lineshape peak parameter  $I_p$  for the free and trapped states, and  $I_w^f$  and  $I_w^t$  are those of the wing parameter  $I_w$  for the free and trapped states, respectively. Here R parameter is independent of concentration and characterizes the type of trapping centers that are present. If several types of trapping sites are available for the positrons at the same time, the above argument is also valid as long as one type of trapping sites predominates.

The life-time and the Doppler broadening accompanying positron annihilation (PA) were measured with use of the PA measuring instruments in the Non-Destructive Test Laboratory of the Korea Standards Research Institute.

The positron annihilation (PA) measurement system has two plastic scintillators mounted on the photomultiplier tubes (PMT). Two constant fraction discriminators (CFDD) were used to discriminate the start and stop signals from the two detectors. The start signal and the delayed stop signal were fed to a time analyzer, and the time duration between the birth and the annihilation of a positron in a specimen was measured by a time analyzer. The measured timing information was sent to the multichannel analyzer (MCA) through an analog-to-digital convert (ADC) to form a time spectrum. The time spectrum was analyzed by a computer using the program that was originally developed at Queen's University, Canada and modified at Brookhaven National

Laboratory in U.S.A. The details of the data analysis are reported elsewhere. [28] The time scale of the system was calibrated using a time calibrator.

The energy of  $\gamma$ -rays was measured with use of a high purity Ge detector of the measurement system. The energy resolution was 1.64 keV full width of half maximum (FWHM) for the fiducial  $\gamma$ -ray of 1.274MeV. The line shape of the Doppler broadened  $\gamma$ -rays measured with use of MCA through a spectroscopy amplifier and an ADC. The line shape was found to be dependent on the counting rate. [28] As the counting rate increases, the line shape becomes broader for the specimen. The variation of the line shape was relatively small when the integrated counting rate (ICPS) was around 250 counts/s. All line shapes in this work were measured with the same counting rate of 250 counts/s.

The life-time distribution, however, is also separated into two portions, namely, one being that due to the annihilation of a positron-free electron pair and the other being that due to the annihilation of a positron-core electron pair. Hence the life-time measuring system must measure separately these two portions and test whether two portions are separated or not.  $^{207}\text{Bi}$  and well-annealed 99.999% Cu were used to check the performance of the life measuring system. The reason why  $^{207}\text{Bi}$  and Cu were used is that they have clearly evident lifetimes, namely, 187 ps for  $^{207}\text{Bi}$  and 157 ps for Cu. As a result analysis must be performed by one-trapped method after source lifetime is determined by analysis of one lifetime component, and source lifetime is set to the result obtained from core-trapped method.

### III. RESULTS AND DISCUSSION

#### III-1. Isochronally Annealed Specimens

##### 1. Microhardness

Fig.3 shows the results of microhardness tests

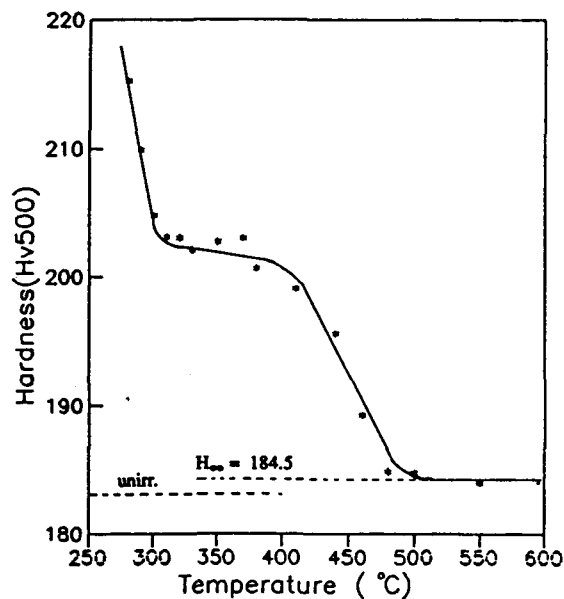


Fig. 3 Microhardness changes of the RPV steel isochronally annealed for 4 hours.

on isochronally annealed specimens. It can be seen from these results that one recovery process occurs in the temperature range of 280–305°C and the other recovery process in the temperature range of 405–490°C. The hardness value scarcely changed for specimens annealed isochronally in the temperature range of 305–405°C. These results seem to indicate that defects of higher activation energy were formed without altering the effective defect density [21] but the hardness value representing the effective defect density varies very slowly in this region. Hence microhardness of specimens annealed in this region can be explained by the compounded effect of radiation anneal hardening (RAH) and recovery by vacancy annihilation.

##### 2. Positron Annihilation (PA) Measurements

Fig.4 and Fig.5 show the Doppler broadening results obtained from specimens annealed for four hours isochronally, namely,  $I_p$  peak parameter and  $I_w$  wing parameter, and R parameter, respectively.

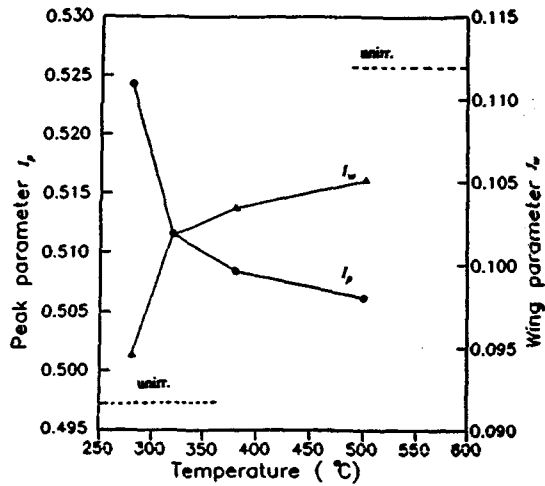


Fig. 4 Variations of the Doppler parameters  $I_p$  and  $I_w$  for the RPV steel isochronally annealed.

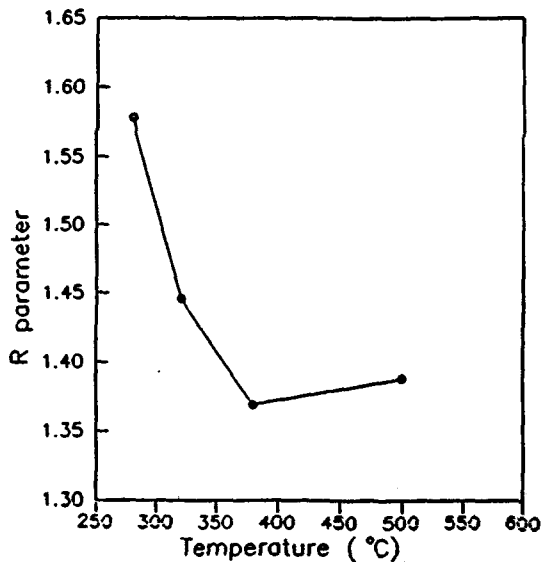


Fig. 5 Variations of the R parameter for the RPV steel isochronally annealed.

They are in good agreement with the results of C.Lopes Gil et al.[23].

The peak parameter  $I_p$  decreased for the specimen isochronally annealed in the temperature range of 280–380°C. This means that the density of vacancy-type defects decreased. While the hardness value decreased, the peak parameter  $I_p$

scarcely changed for the specimen annealed isochronally in the temperature range of 380–500°C. This means that this change was due to that in the density of non-vacancy type defects.

Fig.6 and Fig.7 show the results of positron

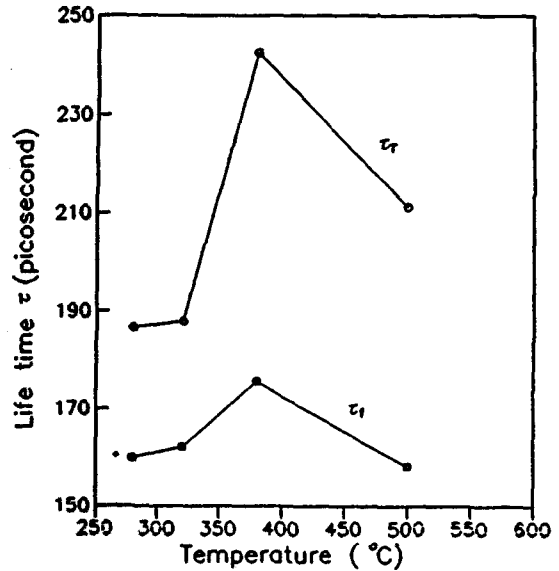


Fig. 6 Variation of the life-times  $\tau_T$  and  $\tau_f$  for the RPV steel isochronally annealed

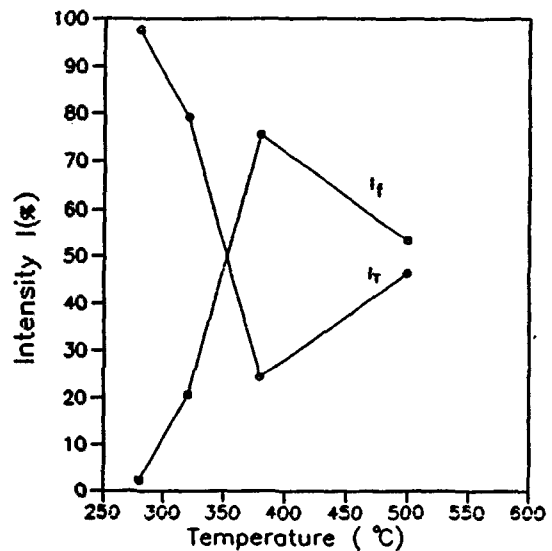


Fig. 7 Variations of the intensities  $I_T$  and  $I_f$  for the RPV steel isochronally annealed.

lifetime and intensity measurements, respectively, where subscript T denotes annihilation of trapped positrons at vacancies and subscript f denotes positron annihilation with the core electrons. The decrease of  $I_T$  for the specimens annealed in the range of 280–320°C seems to indicate that the average dimension of vacancy-type defects increased a little and the total number of defects decreased. The variation of  $I_T$  for the specimens annealed in the range of 320–500°C was similar to the results of the positron annihilation experiment for RPV steel reported by C. Lopes Gil et al. [23]. Drawing a straight line between 320°C data point and 500°C data points, this line is nearly straight with that connecting with 280°C data point. Hence these results seem to indicate that monovacancies were annihilated continuously in the specimens annealed in the whole range of isochronal annealing. The increase of lifetime  $\tau$  and the decrease of intensity  $I$  for specimens annealed in the range of 320–380°C indicate the formation of the vacancy clusters or voids that were decorated by carbon migration, or the precipitation of nitrides. Since the copper content of RPV base metal is low, the role of copper was considered to be negligible. It was reported that isochronal annealing of specimens in the range of 380–500°C causes dissolution to the matrix of decorated carbons at vacancy clusters and precipitates. [16,23]

### 3. Correlation of Microhardness and Positron Annihilation Measurements

Vacancies agglomerate with vacancies, vacancy clusters, or voids in the first stage of isochronal annealing in the temperature range of 280–305°C. [22] Impurity carbons migrate and decorate vacancy-type defects, and/or possibly other impurity precipitates are formed in the temperature range of 305–405°C. [23] Since carbon shells around vacancy-type defects are metastable at higher temperature above 405°C, decorated

carbon atoms are released to the matrix, [18] and other possible precipitates are dissolved. Hence, the defect structure prior to the carbon decoration and possible precipitation is gradually recovered. In the whole temperature range monovacancies appear to be annihilated also at sinks continuously during isochronal annealing. It can be seen from the isochronal annealing curves shown in Fig.3. and Fig.4. that fully recovered steel specimens did not show characteristics exhibited by non-irradiated specimens ( $H=183.25$ ,  $I_p=0.4970$ ,  $I_w=0.1119$ ). [30]

## III-2. Isothermally Annealed Specimens

### 1. Microhardness

Fig.8 shows the results of microhardness tests on specimens isothermally annealed at 380°C.

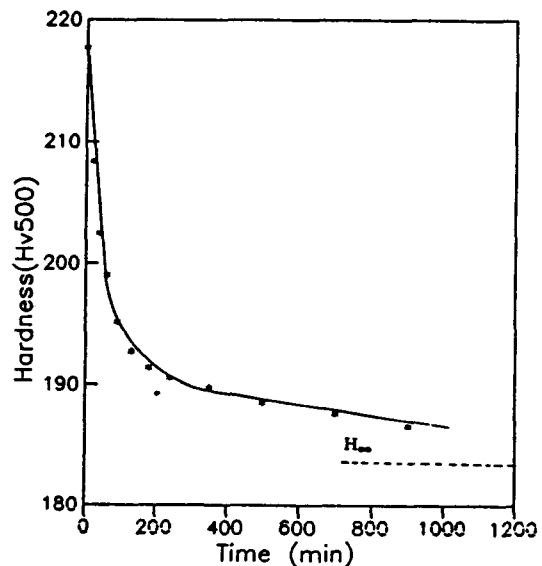


Fig. 8 Microhardness (Hv) changes of the RPV steel isothermally annealed at 380°C.

This figure shows recovery of two stages in the early region and the later region. Detailed recovery processes can not be analyzed by microhardness data alone but can be analyzed in conjunction with the positron annihilation method.

## 2. Positron Annihilation(PA)

The results of Doppler broadening for the specimens isothermally annealed at 380°C are shown in Figs.9 and 10. The results of lifetime measure-

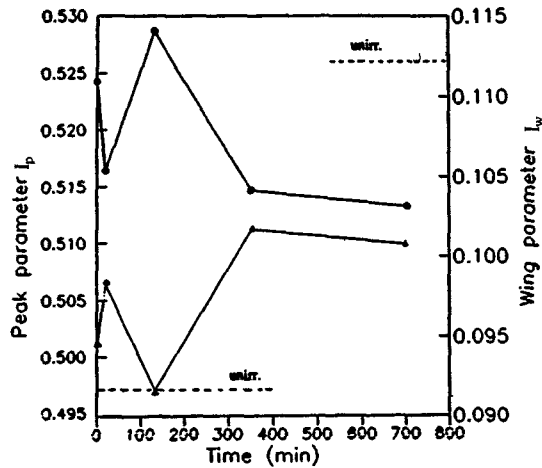


Fig. 9 Variations of the Doppler parameters  $I_p$  and  $I_w$  for the RPV steel isothermally annealed at 380°C.

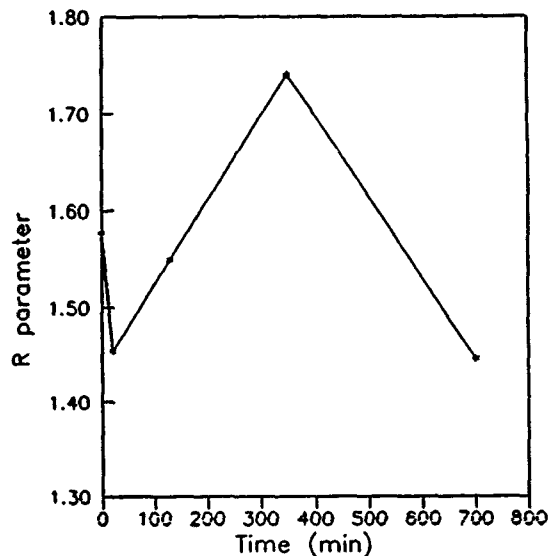


Fig. 10 Variations of the R parameter for the RPV steel isothermally annealed at 380°C.

ments can not be analyzed because of the complication of lifetime analysis for this specimen.

The sharp decrease of peak parameter  $I_p$  and the sharp increase of wing parameter  $I_w$  for the specimen annealed for 0–20 min. at 350°C indicate that free vacancies were annihilated at dislocations or internal sinks. The decrease of R parameter for the specimen annealed for short time also supports this interpretation. The increase of peak parameter  $I_p$  and the decrease of wing parameter  $I_w$  for the specimen annealed for 20–30 min. at 380°C indicate that the size of vacancy-type defects, namely, vacancy clusters and voids was growing by agglomeration of vacancies. The increase of R parameter for the specimen annealed for 20–350 min. indicates that the characters of dominant trapping sites changed. Hence all these parameters support the interpretation that agglomeration of vacancies occurred in the specimens annealed for 20–130 min. Peak parameter  $I_p$  decreased for the specimen annealed for 130–350 min. whereas wing parameter  $I_w$  increased. This observation indicates a decrease of the average dimension of vacancy-type defects by annihilation of monovacancies. R parameter for this specimen, however, increased. Hence, it appears that the agglomeration of vacancies and the decrease of the average dimension occurred simultaneously. The vacancy agglomeration seems to occur mainly in the time interval of 20–130 min. and the decrease of the average dimension seems to occur predominantly in the time interval of 130–350 min. Both parameter  $I_p$  and  $I_w$  were nearly constant for the specimens annealed for a longer time duration than 350 min. It appears that vacancy-type defects were continuously annihilated even after 350 min.

## 3. Correlation of Microhardness and Positron Annihilation Measurements

Free vacancies existing in the specimen seems to move to sinks such as dislocations and internal

sinks in the early stage (up to 20 min) of isothermal annealing at 380°C. It seemed subsequently that the agglomeration of vacancies occur in the specimen during annealing for 20–350 min. and a decrease of the density of vacancy-type defects by vacancy annihilation occur during the entire period of isothermal annealing. Analysis of the variations of  $I_p$ ,  $I_w$  and R parameter indicates that the agglomeration of vacancies occurs predominantly during annealing for 20–130 min. and the decrease of the density of vacancy-type defects occurs predominantly during annealing for 130–350 min.

### III-3. Determination of Activation Energy and Kinetics

#### 1. Determination of Activation Energy

The Meechan–Brinkman method [19] was used to evaluate the activation energies for recovery processes corresponding to decreases in hardness. Activation energies were determined with use of microhardness data of specimens annealed isochronally and isothermally at 380°C. The activation energy for the first recovery stage was determined as 1.76 eV whereas that of the second recovery stage as 2.00 eV. These values are lower than those reported by previous workers [20]. This difference may arise from the fact that the copper content of the RPV in present study was much lower than that of steels used by other workers. Pachur [20] obtained activation energies ranging between 1.5 and 2.5 eV for recovery processes associated with his annealing experiment.

#### 2. Determination of Kinetics

Kinetics was determined by the Meechan–Brinkman method using isothermal annealing data. [19] Here microhardness data of the specimens isothermally annealed at 320°C were used representatively. It was possible to determine first the order of reaction for the second recovery

stage because there was only one recovery mechanism in the second recovery stage. Microhardness data of the second recovery stage were expressed as

$$H_2(t) = H(t) - H_\infty \quad (3)$$

where  $H(t)$  is microhardness data experimentally measured and  $H_\infty$  is completely recovered (asymptote) microhardness. When the plot of  $\ln H$  vs.  $\ln(t+M)$  became a straight-line, the order of reaction ( $\gamma$ ) was determined. For the second stage the slope was determined as  $-1.488$ , the order of reaction as 1.67, and the value of  $M$  as 397 min.  $H_{20}$  (microhardness at  $t=0$  of the specimen in the second recovery stage) was determined as 20.82 from these results. Subsequently, the order of reaction was determined for the first recovery stage. In this case the following relationship hold for microhardness data of the first recovery stage;

$$H_1(t) = H(t) - H_\infty - H_2(t) \quad (4)$$

where  $H_2(t)$  was determined as  $[C_2(t+397)]^{1/(1-1.67)}$  and  $H_{10}$  (microhardness at  $t=0$  of the specimen in the first recovery stage) was 12.39. The same method employed for the second recovery stage yielded the slope as  $-1.276$ , the order of reaction as 1.78, and  $M$  as 21 min.

The order of reaction is generally an integer for a single mechanism or for pure metal. The orders of reactions obtained here were not integers. The results similar to this were observed in other studies. [32] It seems that several mechanisms of the first order and the second order were compounded in one recovery stage. Mechanisms such as agglomeration of vacancies, formation of carbon decorated clusters by carbon migration, annihilation of vacancies seem to be compounded in the first recovery stage, and mechanisms such as annihilation of vacancies, dissolution of decorated carbons and precipitates also seem to occur in the second recovery stage. Since the specimens used in the present study were not a pure metal but an iron-base alloy, non-integer orders of reactions

may be justified.

## V. CONCLUSIONS

The following conclusions are drawn from microhardness and positron annihilation measurements on isochronally and isothermally annealed specimens of RPV steel A533B Cl. 1 base metal radiated with a dose of  $4.84 \times 10^{18}$  n/cm<sup>2</sup> neutrons at about 280°C

1. Positron annihilation (PA) parameters measured indicated that the first recovery of radiation hardening of reactor pressure vessel (RPV) steel during isochronal anneal in the temperature range of 280–305°C is attributed to formation of vacancy clusters by vacancy agglomeration. For the specimens isochronally annealed in the temperature range of 405–490°C, PA parameters indicated that the second recovery process is attributed to the dissolution of carbon atoms decorated around vacancy-type defects and other possible precipitates, and the annihilation of monovacancies from defect surfaces. For the specimens annealed in the mid-temperature range of 305–405°C between the temperature ranges for the two recovery processes, it was indicated that radiation anneal hardening (RAH) is attributed to the formation of carbon decorated vacancy clusters and other possible precipitates.

2. PA parameters for the specimen in the early stage (up to 20 min.) of isothermal anneal at 380°C indicated that free vacancies existing in the specimen move to sinks such as dislocations and other thermal sinks. PA parameters measured indicated that the agglomeration of vacancies occurs predominantly during isothermal annealing for 20–30 min. and the decrease of the density of vacancy-type defects occurs predominantly during further annealing for 130–350 min.

3. The activation energy of the first recovery process was determined as 1.76 eV and that of the second recovery process as 2.00 eV. These values are lower than those obtained by Pachur. This difference may be attributed to the lower copper content of the RPV steel used in the present study.

4. The order of reaction was determined as 1.78 for the first recovery process. On the other hand, the order of reaction was determined as 1.67 for the second recovery process. Non-integer orders of reaction for recovery processes are attributed to the fact that several mechanisms of the first order and second order of reaction are compounded in one process. This results also supports for the first and the second conclusions above.

## REFERENCES

1. U.S. Code of Federal Regulation (CFR), App.G, "Fracture Toughness Requirements", Title 10, Ch.1, 367(1978).
2. G.E. Lucas and G.R. Odette, "Recent Advances in Understanding Radiation Hardening and Embrittlement Mechanism in Pressure Vessel Steels", Proc. of 2nd Inter. Symp. on Environmental Degradation of Materials in Power Systems—Water Reactor, (Monterey, California, Sep. 9–12, 1985), 345–360.
3. E.C. Biemiller and S.T. Byrne, "Evaluation of the Effect of Chemical Composition on the Irradiation Sensitivity of Reactor Pressure Vessel's Weld Material", ASTM STP 611, 418–433(1976).
4. B.L. Shriver, A.P. Main, and D.C. Hicke, "Analytic Predictions of Embrittlement of SA533B Pressure Vessel Steels", ASTM STP 782, 492–504(1982).
5. J.D. Varsik and S.T. Byrne, "An Empirical Evaluation of the Irradiation Sensitivity of

- Reactor Pressure Vessel Materials", ASTM STP 683, 252-266(1979).
6. C. Guionnet, et. al., "Radiation Embrittlement of PWR Vessel Steel: Effects of Impurities and Nickel Content", ASTM STP 725, 20-37(1981).
  7. J.A. Spitznagel, R.P. Shogan, and J.H. Phillips, "Annealing of Irradiation Damage in High Copper Ferritic Steels", ASTM STP 611, 434-448(1976).
  8. C. Leitz, et.al., "Comparative Irradiation Study of Reactor Pressure Vessel Steel Weld Metals", ASTM STP 782, 492-504(1982).
  9. I.M. Robertson, C.A. English, and M.L. Jenkins, "Dissolution of Nitride Precipitates in Iron by Low Dose Neutron Irradiation", *Radia. Effec.*, Vol.102(1987), 53-68.
  10. Michio Kiritani and Hiroshi Takata, "Dynamic Studies of Defect Mobility Using High Voltage Electron Microscopy", *J. Nucl. Mater.*, Vol.69&70(1978), 277-309.
  11. R.W. Balluffi, "Vacancy Defect Mobilities and Binding Energies Obtained from Annealing Studies", *J. Nucl. Mater.*, Vol.69&70(1978) 240-263.
  12. A. Vehanen, et.al., "Vacancies and Carbon Impurities in  $\alpha$ -iron: Electron Irradiation", *Physical Review B*, Vol.25, No.2, 762-780(1982).
  13. C.C. Dollins, "Post Irradiation Recovery of Copper Alloys after Neutron Irradiation at Low Temperature", *Radiation Effects*, Vol.17(1973) 151-158.
  14. K. Ghazi-Wakili, et.al., "Positron Annihilation Studies on Neutron Irradiated Pressure Vessel Steels", *Phys. Stat. Sol.(a)*, Vol.102(1987), 153-164.
  15. D.J. Harvey and M.S. Wechsler, "Kinetics of Annealing of Irradiated Surveillance Pressure Vessel Steel", ASTM STP 782, 492-504(1982).
  16. B.S. Viswanathan, D. Pachur, and R.V. Nandedkar, "Investigation of Neutron Irradiated Reactor Pressure Vessel Steel by Positron Annihilation and Electron Microscopy", ASTM STP 956, 369-378(1987).
  17. W. Primak, "Kinetics of Processes Distributed in Activation Energy", *Physical Review*, Vol.1000, No.6, 1677-1689(1955).
  18. W.Primak, "Fast-Neutron Damaging in Nuclear Reactors: Its Kinetics and the Carbon Atom Displacement Rate", *Physical Review*, Vol.103, No.6, 1681-1692(1956).
  19. C.J. Meechan and J.A. Brinkman, "Electrical Resistivity Study of Lattice Defects Introduced in Copper by 1.25 MeV Electron Irradiation at 80°K", *Physical Review*, Vol.103, No.5, 1193-1202(1956).
  20. D. Pachur, "Radiation Annealing Mechanisms of Low-Alloy Reactor Pressure Vessel Steels Dependent on Irradiation Temperature and Neutron Fluence", *Nuclear Technology*, Vol.59(1982) 463.
  21. D. Pachur, "Apparent Embrittlement Saturation and Radiation Mechanism of Reactor Pressure Vessel Steels", ASTM STP 725, 5-19(1981).
  22. Y.K. Park, J.O. Lee and S.K. Lee, "Nondestructive Characterization of a Deformed Steel Using Positron Annihilation", 3rd International Conference of Nondestructive Characterization of Materials, Saarbrucken, Oct. 1988.
  23. W. Brandt and R. Paulin, "Positron Annihilation Profile Effects in Solid", *Physical Review B*, Vol.15, No.5(1977).
  24. R.M. West: *Positron Studies of Lattice Defects in Metals*, *Positrons in Solid*, ed. P. Hautojarvi, Springer-Verlag(1979) 89-144.
  25. R.M. Nieminen and M.J. Manninen, "Positrons in Imperfect Solids: Theory", *Positrons in Solid*, ed. P. Hautojarvi, Springer-Verlag(1979) 145-195.
  26. W. Brandt, "Positron as a Probe of the Solid State", *Scientific American*, Vol.233(1975),

- 34-42.
7. P. Hautojarvi and A. Vehanen, "Introduction to Positron Annihilation", Positrons in Solid, ed. P. Hautojarvi, Springer-Verlag(1979) 1-23.
  8. Y.K. Park : Determination by Positron Annihilation and Electrolytic Hydrogen Permeation of the Dislocation and Hydrogen Trap Densities in Annealed and Deformed Pure Iron Single Crystal, Ph.D. Thesis, 1985, Northwestern University, Illi., U.S.A.
  9. C.Lopes Gil, et.al., "Neutron Irradiated Reactor Pressure Vessel Steels Investigated by Positron Annihilation", J. Nucl. Mater., Vol.161(1989), 1-12.
  30. K. Kussmaul, J. Fohl, and T. Weissenberg, "Investigation of Materials from Decommissioned Reactor Pressure Vessel—a Contribution to the Understanding of Irradiation Embrittlement", ASTM 14th Inter. Symp. on Effects of Radiation on Materials, Andover, USA, ASTM, June27-29(1988).
  31. S. Mantl and W. Triftshauser, "Direct Evidence for Vacancy Clustering in Electron Irradiated Copper by Positron Annihilation", Physical Review Letters, Vol.34, No.25, 1554-1557(1975).
  32. A.L. Overhauser, "Isothermal Annealing Effects in Irradiated Copper", Physical Review, Vol.90, No.3, 393-400(1953).